Modeling of the radiative process in an atmospheric general circulation model

Teruyuki Nakajima, Masahito Tsukamoto, Yoko Tsushima, Atusi Numaguti, and Toshiyoshi Kimura

A new radiation scheme has been developed for dynamic general-circulation modeling. An automatic determination of k-distribution parameters and a treatment of solar–terrestrial radiation interacting with gaseous and particulate matter are incorporated into the scheme by a technique that combines discrete ordinate and matrix operator methods. An accelerated scheme for cloud overlap is developed and tested. The resultant accuracy of the scheme is ± 0.5 K/day to a 70-km height in clear sky better than that of the line-by-line calculation method. © 2000 Optical Society of America

OCIS codes: 010.3920, 030.5620, 300.1030, 290.1090.

1. Introduction

Modeling of radiation in the Earth's atmosphere is an important component in numerical climate modeling, especially for long-term climate simulations. Several important processes must be included in the radiation code. Gaseous absorption, including that of greenhouse gases, has to be treated accurately. It is also important to include scattering, absorption, and emission of radiation by particulate matter, such as clouds and aerosols, in the model. There has been considerable effort to make fast yet comprehensive radiation codes that can treat these processes with k-distribution approximation.[1–3] Although there is progress toward improving band-model schemes,[4] use of k-distribution methods seems more promising than band models for climate studies. In k-distribution methods the cloud emissivity can be calculated by the model itself, so there is no approximation for partial emissivity for thin clouds. Moreover, the amount of computation is proportional to the number of vertical levels N, compared with N^2 in most band models. There are, however, still several drawbacks that must be overcome before this powerful method can be adopted for use in general-circulation models (GCM's). We need many equivalent wavelengths, or channels, to calculate accurate radiative fluxes, especially for evaluation of overlapping band absorption with several gas species.

In this paper we propose a new radiation code for an atmospheric general-circulation model. This code combines a k-distribution method with the discrete ordinate method/adding the method of Nakajima and Tanaka.[5] We have overcome several of the serious problems mentioned above for k-distribution methods by adopting a new technique for minimizing objectives of equivalent channels for k distribution. Treatment of the radiative effect of particulate matter and the overlap effect of partial cloud layers is also discussed.

The first version of the code was developed in 1995. Since then the performance of the radiation code has been confirmed by several GCM's and mesoscale models implemented with that code.

2. Formulation of the Radiative Transfer

The radiative transfer equation for diffuse radiation u in a plane-parallel homogeneous atmosphere at a monochromatic wavelength is given by

$$\begin{aligned}\mu \frac{\mathrm{d}u(\tau, \mu, \phi)}{\mathrm{d}\tau} = &-u(\tau, \mu, \phi) \\ &+ \omega \int_{-1}^{1} \mathrm{d}\mu' \int_{0}^{2\pi} \mathrm{d}\phi' P(\mu, \mu', \phi \\ &- \phi') u(\tau, \mu', \phi') \\ &+ \omega P(\mu, \mu_0, \phi) \exp(-\tau/\mu_0) F_0 \\ &+ (1 - \omega) B(\tau), \end{aligned} \tag{1}$$

The authors are with the Center for Climate System Research, University of Tokyo, 4-6-1 Komaba, Meguro-ku, Tokyo 153-8904, Japan. M. Tsukamoto is deceased. The e-mail address for T. Nakajima is teruyuki@ccsr.u-tokyo.ac.jp.

Received 23 July 1999; revised manuscript received 11 April 2000.
0003-6935/00/274869-10$15.00/0

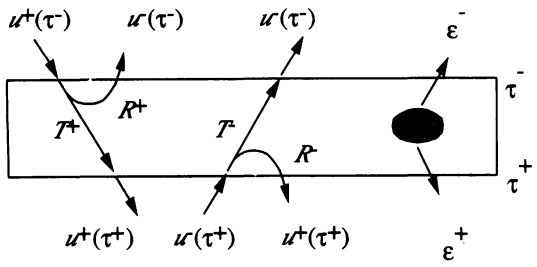

Fig. 1. Matrix operators that characterize the radiative process in a homogeneous layer.

where τ is the optical depth, μ is the cosine of the nadir angle of the propagation direction of the ray, ϕ is the azimuthal angle of the propagation direction measured from the solar plane, μ_0 is the cosine of the solar zenith angle, ω is the single-scattering albedo, $P(\mu, \mu', \phi - \phi')$ is a scattering phase function that represents single scattering from directions (μ', ϕ') to (μ, ϕ), F_0 is the solar incident irradiance at the top of the atmosphere, and $B(\tau)$ is a Planck function. The following matrix equation is obtained[5] if we quantize the μ axis and expand Eq. (1) into a Fourier series for ϕ:

$$\pm\mathbf{M}\frac{\mathrm{d}\mathbf{u}^{\pm}(\tau)}{\mathrm{d}\tau} = -\mathbf{u}^{\pm}(\tau) + \mathbf{P}^{\pm}\mathbf{W}\mathbf{u}^{+}(\tau) + \mathbf{P}^{\mp}\mathbf{W}\mathbf{u}^{-}(\tau) + \mathbf{S}_{\mathbf{S}}^{\pm}\exp(-\tau/\mu_0) + \mathbf{S}_{\mathbf{B}}(\tau), \tag{2}$$

where vectors and matrices are defined as

$$\mathbf{u}^{\pm} = \left[\int_0^{2\pi} u(\tau, \pm\mu_i, \mu_0, \phi)\cos m\phi \mathrm{d}\phi | \mathrm{i}=1, \mathrm{N}\right], \tag{3}$$

$$\mathbf{P}^{\pm} = \left[\omega\int_0^{2\pi} P(\pm\mu_i, \mu_j, \phi)\cos m\phi \mathrm{d}\phi | \mathrm{i}, \mathrm{j}=1, \mathrm{N}\right], \tag{4}$$

$$\mathbf{S}_{\mathbf{S}}^{\pm} = \left[\omega\int_0^{2\pi} P(\pm\mu_i, \mu_0, \phi)\cos m\phi \mathrm{d}F_0 | \mathrm{i}=1, \mathrm{N}\right], \tag{5}$$

$$\mathbf{S}_{\mathbf{B}}^{\pm} = [2\pi\delta_{0m}(1-\omega)B(\tau)|i = 1, N], \tag{6}$$

$$\mathbf{M} = [\mu_i\delta_{ij}|i = 1, N]; \qquad \mathbf{W} = (w_i\delta_{ij}|i = 1, N), \tag{7}$$

where m is the order of Fourier series and $\{\mu_i, w_i\}$ are the points and weights for a discrete quadrature of order N in the hemisphere. In Eqs. (2)–(7), + means downward propagation and $\neg$ means upward propagation.

We can solve Eq. (2) by reducing the problem to an eigenvector decomposition problem of finding the reflection, transmission, and source matrices for a homogeneous layer, as was shown by Nakajima and Tanaka.[5] The matrix operators for the layer can be defined as transform operators of scaled radiances (see Fig. 1):

$$\mathbf{u}^{\pm}(\tau^{\pm}) \equiv \sqrt{\mathbf{w}\boldsymbol{\mu}}\mathbf{u}^{\pm}(\tau^{\pm}) = \mathbf{R}^{\mp}\mathbf{u}^{\mp}(\tau^{\pm}) + \mathbf{T}^{\pm}\mathbf{u}^{\pm}(\tau^{\mp}) + \boldsymbol{\varepsilon}^{\pm}, \tag{8}$$

where τ^- and τ^+ are optical depths at the top and bottom, respectively, of the layer. T, R, and $\varepsilon^{\pm}$ are the scaled reflection and transmission matrices and the emission vector, respectively.

These operators can be expressed in terms of quantities for single scattering. In the case of a two-stream approximation ($N = 1$, $\mu_i = \mu$, $w_i = w$) the matrices that appear in these expressions become scalars, so we can commute any combination of matrices in the solution. The expressions for reflection and transmission matrices can be summarized as in Appendix A. In the expressions we need the first three moments of the phase function expanded into a series of Legendre polynomials:

$$P(x) = \sum_{n=0}^{N}\frac{2n+1}{4\pi}g_nP_n(x). \tag{9}$$

The first moment is trivial, from the normalization condition of the phase function, and second and third moments are referred to as the asymmetry factor and the truncation factor, respectively, in the delta two-stream approximation[6]:

$$g_0 = 1, \quad g = g_1, \quad f = g_2. \tag{10}$$

We introduce the delta two-stream truncation and redefine truncated quantities as follows:

$$\tau \leftarrow (1-\omega f)\tau, \quad \omega \leftarrow \frac{1-f}{1-\omega f}\omega, \quad g \leftarrow \frac{g-f}{1-f}. \tag{11}$$

In this approximation the truncated phase function is given as

$$P^{(0)}(\pm\mu, \mu') \equiv \int_0^{2\pi} P(\pm\mu, \mu', \phi)d\phi = \tfrac{1}{2}(1 \pm 3g\mu\mu'). \tag{12}$$

We need only the zeroth-order Fourier term to calculate radiative fluxes.

To take into account the effect of thermal emission we expand the Planck function into polynomials of the optical depth[7]:

$$B(\tau) = \sum_{n=0}^{N_b} b_n(\tau - \tau^-)^n. \tag{13}$$

In the truncation approximation we need the following replacement for the expansion coefficients:

$$b_n \leftarrow \frac{b_n}{(1-\omega f)^n}. \tag{14}$$

Appendix A gives detailed expressions for source matrices with this expansion. We adopted $N_b = 2$ to eliminate the two-grid noise in the heating rate profile that occurs as the coupling of dynamics and radiative processes in the linear expansion approximation.

With respect to particulate matter, we prepared optical parameters of seven species, i.e., water cloud, ice cloud, dustlike aerosol, water-soluble aerosol, oce-

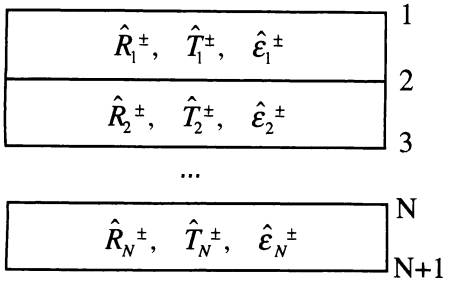

Fig. 2. System of sublayers as an approximation of an inhomogeneous atmosphere.

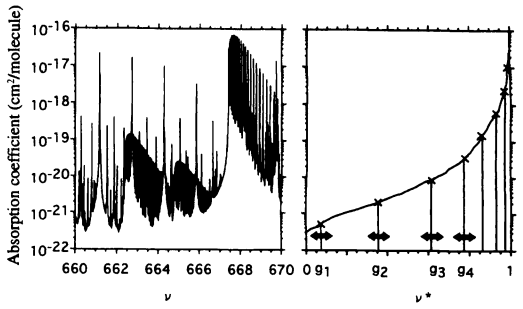

Fig. 3. Concept of k distribution.

anic aerosol, soot aerosol, volcanic ash, and 75% H_2SO_4 aerosol. The optical parameter table for particulate matter contains

$$e = C_{\text{ext}}/V, \quad s_0 = C_{\text{sca}}/V, \quad s_1 = C_{\text{sca}} g_1/V, \ldots, \quad s_4 = C_{\text{sca}} g_4/V \tag{15}$$

for each species. The first parameter is the extinction coefficient per unit volume of particulate matter. The other five parameters are moments of the volume scattering phase function, $C_{\text{sca}}P(\Theta)/V$. We prepared moments up to fourth order to take into account the use of a four-stream model for some applications. Given the volume of each particulate species and the geometric thickness of the sublayer, we calculated the truncated optical thickness and the single-scattering albedo from Eqs. (15) and relations (11). Optical thicknesses for extinction and for scattering are calculated from the volume of each particulate as

$$\tau_P = \sum_{m=1} \exp[{}^{(m)}V^{(m)}], \tag{16}$$

$$\sigma_{P,n} = \sum_{m=1} s_n^{(m)} V^{(m)}, \tag{17}$$

where m means the polydispersion species number.

The single-scattering albedo and the phase-function moments are calculated from Eqs. (16) and (17) as

$$\omega_P = \sigma_{P,0}/\tau; \qquad g_{P,n} = \sigma_{P,n}/\sigma_{P,0}. \tag{18}$$

Approximating the atmosphere by a set of homogeneous sublayers (Fig. 2), we can obtain operators for each sublayer by applying the formula mentioned above. Radiative fluxes at the interfaces of sublayers can be obtained from the regular adding theory[8] applied to the scaled variables used in our formulation. The expression for the internal field is as given in Appendix B, and the heating rate is calculated from this internal field. As for the value of the discrete quadrature (μ, w) for the two-stream approximation, we adopted ($1/\sqrt{3}$, 1) and (1/1.66, 1) for short-wave and long-wave spectral regions, i.e., $\lambda < 4$ μm and $\lambda \geq 4$ μm, respectively. In other words, we have adopted the delta two-stream Gaussian approximation and the diffusivity-factor approximation for short-wave and long-wave regions, respectively (see Ref. 9 for definitions of the words). In the long-wave region, thermal emission dominates the scattering process, and, in this case, the diffusivity-factor approximation is more accurate than the two-stream Gaussian approximation for estimating the following integral in the transfer solution:

$$\int_0^1 \exp(-x/\mu)\mu \mathrm{d}\mu \approx \tfrac{1}{2} \exp(-x/d), \qquad d \approx 1.66. \tag{19}$$

This means that the following transformation of μ and flux F makes the transfer solution equivalent to the two-stream quadrature formula:

$$\mu \to 1/d, \qquad F \to \pi u. \tag{20}$$

Finally, we have the radiative flux at an optical depth τ:

$$F^{\pm} = \mu w u^{\pm} + \mu_0 \exp(-\tau/\mu_0) F_0, \qquad \lambda < 4\ \mu\text{m}, \tag{21a}$$

$$F^{\pm} = \pi u^{\pm}, \qquad \lambda \geq 4\ \mu\text{m}, \tag{21b}$$

where $u^{\pm} = u^{\pm}/\sqrt{\mu w}$ is the zeroth-order Fourier term for the radiance as defined in Eq. (3).

3. Modeling the Atmospheric Optical Properties

We treat the gas absorption with a k-distribution approximation.[1,10] The absorption coefficients k_ν at regular wave-number grids in a spectral band (ν_A, ν_B) are sorted in order of magnitude to yield the monotonic function $k(\nu^*)$:

$$k_\nu \to k(\nu^*). \tag{22}$$

The function $k(\nu^*)$ is the k distribution, as illustrated in Fig. 3.

If other optical parameters, such as particulate extinction and scattering coefficients and the Planck function, are constant over this band, the following wave-number integrals of the spectral flux are equal:

$$\langle F \rangle = \frac{1}{\nu_B - \nu_A} \int_{\nu_A}^{\nu_B} F_\nu \mathrm{d}\nu = \frac{1}{\nu_B - \nu_A} \int_{\nu_A}^{\nu_B} F(\nu^*) \mathrm{d}\nu^* = \int_0^1 F(g) \mathrm{d}g, \tag{23}$$

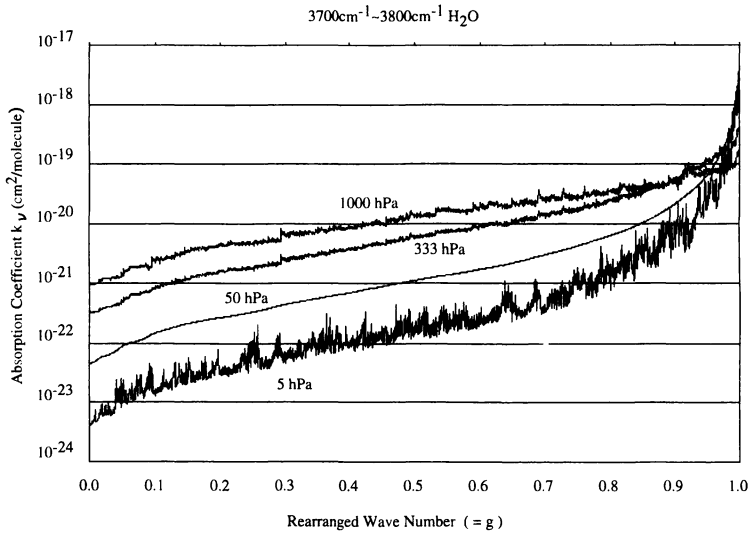

Fig. 4. Sorting of absorption coefficients. Water-vapor absorption in the spectral range of 3700–3800 cm^{-1} is taken as an example. The key sorting wave number is that for $P = 50$ hPa. (Reproduced from Ref. 10).

where the normalized frequency distribution, which is the inverse function of the k distribution, is defined as

$$g(k) = \frac{\nu^*(k) - \nu_A}{\nu_B - \nu_A}. \tag{24}$$

Because the sorted spectrum is a smooth function of ν^* or g, a discrete quadrature of reasonably small order, (k_n, w_n), can be introduced to approximate Eq. (23):

$$\langle F \rangle \approx \sum_{n=1}^{K} F(k_n) w_n, \tag{25}$$

where w_n is a discrete quadrature weight for the nth quadrature wave-number point $\nu_n{}^*$. k_n is given as $k(\nu_n{}^*)$.

The sorted spectrum, $k(\upsilon^*)$, is also a function of pressure and temperature, P and T, respectively, of the ambient atmosphere; hence k_n is also a function of P and T:

$$k_n = k_n(P, T). \tag{26}$$

When we reorder a spectrum at P and T with a sorting key variable ν^* at a standard condition, P_0 and T_0, we find an irregular fine structure in the resultant spectrum unless $P = P_0$ and $T = T_0$, as shown in Fig. 4, which is reproduced from Ref. 10. This means that the assumption of the correlated k-distribution approximation[1] is not valid in real atmospheres. If we sort the absorption coefficients under different (P, T) conditions independently, rays of different colors are mixed in a k-distribution channel, and the monochromatic property of the rays is destroyed. As was shown by Shi,[10] however, this breakdown of the monochromatic property can be ignored in evaluating band-averaged fluxes as a result of cancellation of the fine structure in the course of integration. Therefore we conclude that the correlated k-distribution assumption can be adopted in our study. To keep the monochromatic property of the ray in the k-distribution theory, we must pose a condition that quadrature weights w_n not depend on P and T. This is the most distinct difference from the exponential sum fitting transmissions method,[11] which optimizes $[(k_n, w_n)|n = 1, N]$ without consideration of the monochromatic property of rays.

Under the correlated k-distribution approximation we can estimate $k_n(P, T)$ of each sublayer from a prepared set of $k_n(P_i, T_j)$ at grid points (P_i, T_j). For atmospheres with only one constituent, this approach is enough to permit the integrated flux in each band to be calculated. There are, however, overlapping absorption bands that have more than two gas species, such as the bands of water vapor and CO_2 near 15 μm. Suppose that we have two gaseous components. If there is no correlation in the magnitude of the gaseous absorption coefficients $k^1(\upsilon)$ and $k^2(\upsilon)$ we have to calculate $K_1 \times K_2$, where K_1 and K_2 are the orders of discrete quadrature for gases 1 and 2, respectively, and are possible combinations of absorption coefficients for estimating the band-integrated flux. If the absorption coefficients are completely correlated, however, we have only $K_1 = K_2$ combinations. The real situation lies between these extreme cases. We illustrate this problem schematically in Fig. 5.

We have used this idea to obtain the optimum quadrature $[(k_n, w_n)|n = 1, K]$ for overlapping bands by searching for a solution to minimize a score function for estimating an internal radiation field. The monochromatic condition is interpreted as that in which g_n and w_n do not depend on (P, T) and the k distribution is evaluated as

$$k_n = k^*(g_n). \tag{27}$$

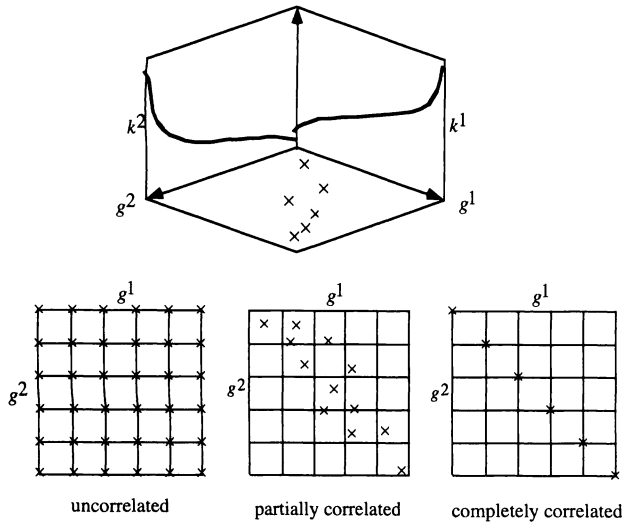

Fig. 5. Treatment of overlapping band absorption for two gases in the k-distribution method.

As for the score function, we try to minimize the error in both flux and heating rates:

$$S(P, T) = c_1\langle(F^+ - F^+_{\text{true}})^2 + (F^- - F^-_{\text{true}})^2\rangle + c_2\langle(H - H_{\text{true}})^2\rangle, \tag{28}$$

where H is the heating rate:

$$H(z) = \frac{1}{C_p\rho}\frac{\mathrm{d}}{\mathrm{d}z}[F^+(z) - F^-(z)]. \tag{29}$$

Weighting coefficients were set as $c_1 = 10^4$ and $c_2 = 10^2$ after some trial and error. We applied a nonlinear optimization called the successive-quadrature program to find the optimum combinations of $\{g_n, w_n\}$ from all possible combinations $\{g_n{}^m, w_n{}^m\}$ with sufficiently large values of K under the assumption of uncorrelated overlapping bands. Starting from this large set with the predetermined number of channels, we used the nonlinear optimizer to search for the optimal set $\{g_n, w_n\}$ within the least margin of error. Let us define "band" as a spectral region for each discrete quadrature $\{k_n, n = 1, K\}$ and "channel" as each quadrature point k_n. The number of channels is determined, after some trial and error, by consideration of the required error budget and computational resources.

We adopted all six U.S. Air Force Geophysics Laboratory (AFGL) atmospheric models under clear-sky conditions as model atmospheres with which to calculate the score function in Eq. (28). For line-by-line calculation of absorption coefficients, we adopted the code designed by Uchiyama[12] with the AFGL HITRAN92 line absorption database. Figure 6 shows the optimized g_n^1 and g_n^2 for water vapor and CO_2 for the 550–770-cm^{-1} spectral range. The location of the frequency distribution in the figure suggests that use of a partial correlation rather than assuming an uncorrelated condition is more suitable for simulating the overlapping band absorptions in this example. However, because we start optimization from completely correlated assumption, the results tend to be on the diagonal line. We accept the resultant parameter combinations as effective, rather than realistic, for minimizing the approximation error in the discrete space.

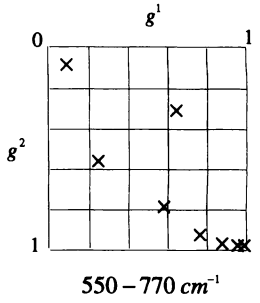

Fig. 6. Optimized frequency distributions for overlapping bands of water vapor and CO_2 in the spectral range 550–770 cm^{-1}.

Because Uchiyama's code is consistent with the definition of line wing cutting of the AFGL LOWTRAN/MODTRAN for treating line absorption (25 cm^{-1} from line center), we adopted the continuum absorption models of AFGL LOWTRAN-6 and LOWTRAN-7,[13,14] including the water-vapor continuum proposed by Clough *et al.*[15] The optical thicknesses for continuum gas absorption are refitted as in the following form:

$$\tau_{O_2} = A^{O2}\rho\Delta z, \tag{30}$$

$$\tau_{O_3} = \sum_{n=0}^{2} A_n^{O3}(T/T_0)^n\rho r^{O3}\Delta z, \tag{31}$$

$$\tau_{H_2O} = [A^{H_2O} + B^{H_2O}(T)r^{H_2O}]r^{H_2O}\rho\Delta z, \tag{32}$$

where r is the gas volume mixing ratio, ρ is the air density at standard conditions $P_0 = 1013$ hPa and $T_0 = 273.2$ K. The absorption of 16 species of chlorofluorocarbons (CFC) is adopted from Shi[16]:

$$\tau_{CFC} = \sum_{n=1}^{16} A_n{}^{CFC} r_n{}^{CFC}\rho\Delta z. \tag{33}$$

Finally, the total optical thickness for the continuum absorption is

$$\tau_{CON} = \tau_{H_2O} + \tau_{O_3} + \tau_{O_2} + \tau_{CFC}. \tag{34}$$

4. Implementation of the Algorithm into a General-Circulation Model

Applying the method proposed above, we made two versions of the radiation code for several atmospheric top heights. A 13-band, 58-channel version (51 for the IR and 7 for the visible–UV) has a model top height of 70 km, and a 13-band, 37-channel version (30 for IR and 7 for visible–UV) has a top height of 40 km. Tables 1 and 2 show the band and channel allocations for these versions. More channels are necessary in the IR region, especially for CO_2 bands, for better accuracy for larger model's top heights. For computational efficiency we fitted $k_n(P_i, T_j)$ at

Table 1. Band and Channel Allocation for a High-Resolution Model

Band	Limit	Channel	Gas
Version H (0–70 km)			
1	50–250	7	H_2O
2	250–400	6	H_2O
3	400–550	4	H_2O
4	550–770	9	H_2O, CO_2
5	770–990	2	H_2O
6	990–1100	5	H_2O, O_3
7	1 100–1400	3	H_2O, N_2O, CH_4
8	1 400–2000	3	H_2O
9	2 000–2500	1	H_2O
10	2 500–4000	5	H_2O
11	4 000–14500	6	H_2O
12	14 500–30000	1	—
13	30 000–50000	6	O_2, O_3
Total		57	

grid points (P_i, T_j) with polynomials of P and T to interpolate $k_n(P, T)$ at arbitrary P and T rather than using a look-up table method. The optical thickness for gaseous line absorption is thus given as

$$\tau_{\mathrm{KD}} = \sum_{m=1} k^{(m)} C_m, \tag{35}$$

with

$$k^{(m)} = \exp\left[\sum_{i=0} \sum_{j=0} A_{ij}^{(m)} (\ln P)^i (T - T_0)^j\right], \tag{36}$$

where C_m is the number of molecules for the mth gas species. From Eqs. (16)–(18), (30), and (34)–(36), the optical parameters for an air mass with gaseous and particulate matter are

$$\tau = \tau_P + \tau_R + \tau_{\mathrm{CON}} + \tau_{\mathrm{KD}}, \tag{37}$$

$$\omega = (\omega_P \tau_P + \omega_R \tau_R)/\tau, \tag{38}$$

$$g_n = (\omega_P \tau_P g_{P,n} + \omega_R \tau_R g_{R,n})/(\omega_P \tau_P + \omega_R \tau_R), \tag{39}$$

Table 2. Band and Channel Allocation for a Low-Resolution Model

Band	Limit	Channel	Gas
Version L (0–37 km)			
1	50–250	3	H_2O
2	250–400	3	H_2O
3	400–550	3	H_2O
4	550–770	6	H_2O, CO_2
5	770–990	2	H_2O
6	990–1100	2	H_2O, O_3
7	1 100–1400	2	H_2O, N_2O, CH_4
8	1 400–2000	1	H_2O
9	2 000–2500	1	H_2O
10	2 500–4000	2	H_2O
11	4 000–14500	5	H_2O
12	14 500–30000	1	—
13	30 000–50000	6	O_2, O_3
Total		37	

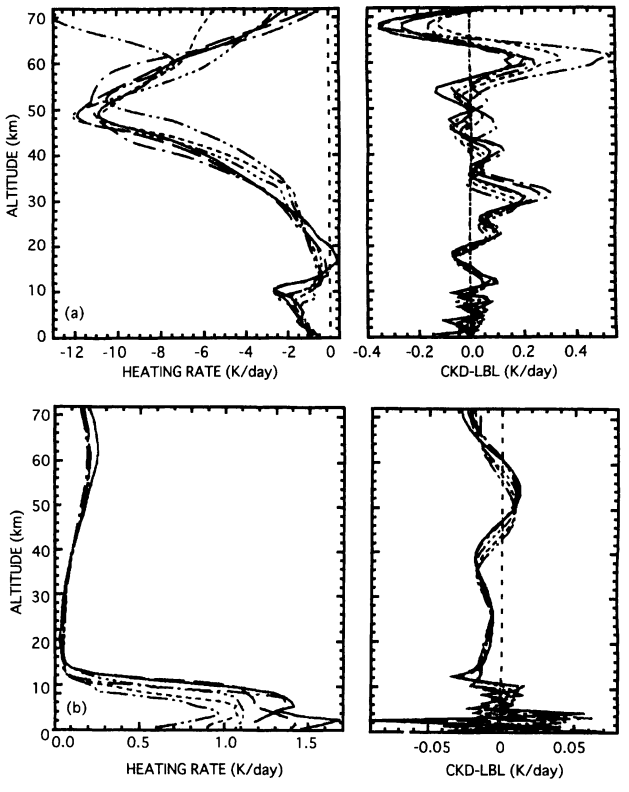

Fig. 7. (a) Vertical profiles of heating rate and error for calculating long-wave flux. (b) Same as in (a) but for the near-infrared region. Six AFGL atmospheres and clear-sky conditions are assumed. ———, tropical; — — —, mid-latitude summer; - - - - - - - -, mid-latitude winter; — — — — — — —, Subarctic summer; — — — — —, subarctic winter; — — — — —, U.S. Standard.

where τ_R, ω_R, and $g_{R,n}$ are the optical thickness, the single-scattering albedo, and the phase-function moments for Rayleigh scattering. We can set $\omega_R = 1$ with enough accuracy to include the Earth's atmosphere. Band-averaged quantities for Rayleigh scattering can be obtained from the well-known values.

Figures 7(a) and 7(b), respectively, show heating-rate and error profiles for the long-wave and the near-IR (NIR) regions. At levels lower than 20 km the error in the heating rate is less than 0.1 K, which is comparable with the results of Fu and Liou.[3]

Implementation of random overlapping of a multilayered cloud system may be one of the troublesome parts of radiation coding for dynamic use. The number of combinationss of overlap is 2^N for an N-layer system, even if we neglect partial cloudliness. With partial cloudliness, computation of these cases is prohibitively time-consuming in the random method. To avoid this problem, we adopt a method, called the semirandom method, that is similar to the clever one proposed by Morcrette and Fouquart,[17] with which we can take advantage of the adding method of radiative transfer adopted in our algorithm. Consider the situation of partially cloudy sublayers with cloud fraction n, as shown in Fig. 8. To approximate the

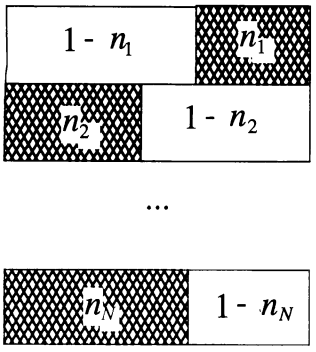

Fig. 8. System of partial cloud layers.

situation, we make the following linear combination operators for each sublayer:

$$\ll R_k \gg, \qquad \ll T_k \gg, \tag{40}$$

where the averaging operator ⟨ths⟩ is defined as

$$\ll Q \gg = nQ_c + (1 - n)Q_s, \tag{41}$$

with subscript c for cloudy conditions and s for clear sky.

The average optical depth at the sublayer top is calculated as

$$\ll t_{1,k} \gg = \prod_{k=1}^{K} \ll t_k \gg, \tag{42}$$

where the transmissivity of the atmosphere for direct solar radiation is defined as

$$t = \exp(-\tau/\mu_0). \tag{43}$$

As in Eq. (A11) below, the source vector of a sublayer can be decomposed into two components, $\varepsilon_{S,k} t_{1,k}$ and $\varepsilon_{B,k}$, which correspond to terms with a solar radiation source and with a thermal radiation source, respectively. We define the average source vector for the system as follows:

$$\ll \varepsilon_k \gg = \ll \varepsilon_{B,k} \gg + \ll \varepsilon_{S,k} \gg \ll t_{1,k} \gg. \tag{44}$$

With those averaged operators given in expression (40) and Eq. (44) for each sublayer, we apply the adding theory given in Appendix B to find the internal field of the partially cloudy system.

Figure 9 shows heating-rate profiles of an atmosphere that has cloud decks located with 2-, 6-, and 9-km cloud-top heights and 1-km thickness for three cases of total cloud fraction: $n = 0, 0.2, 1$. For $n = 0.2$ we assumed a situation of random overlap. The figure shows that the effect of partial cloudiness is more important in the short-wave region than in the long-wave region. Figure 10 shows a comparison of the random and the semirandom methods for other

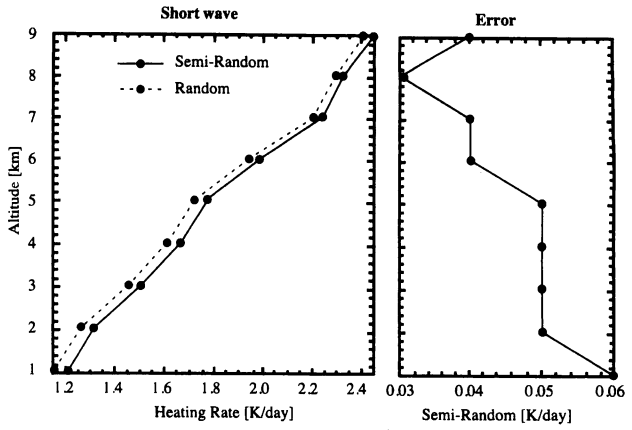

Fig. 10. Heating-rate and error profiles for a partial cloud system calculated by random and semirandom methods.

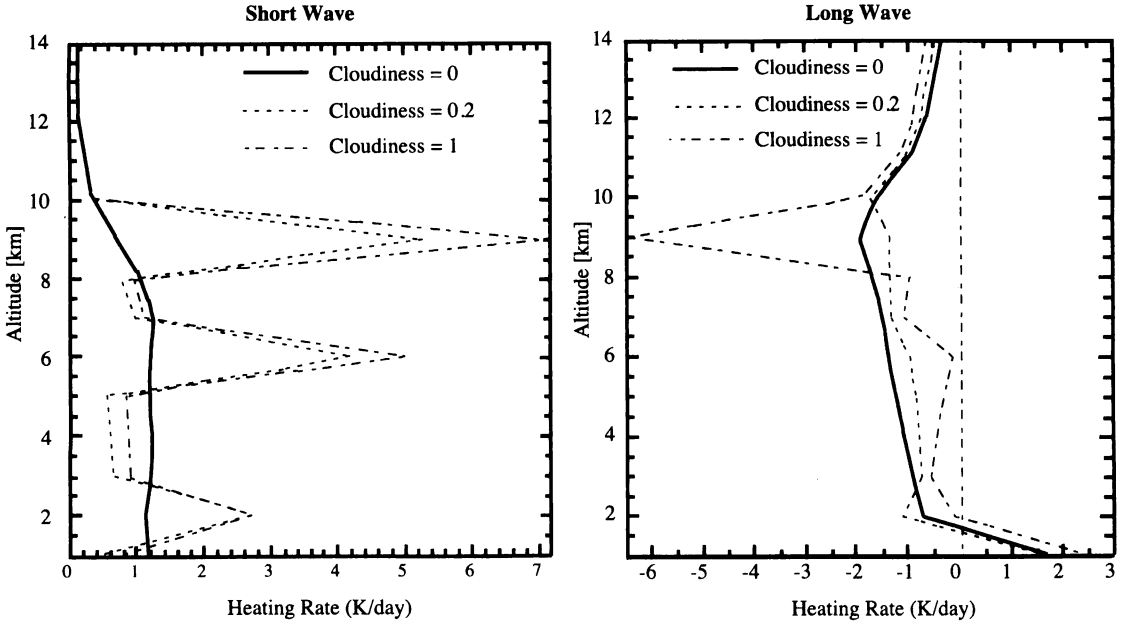

Fig. 9. Heating-rate profiles for atmospheres with clouds located at 2, 6, and 9 km.

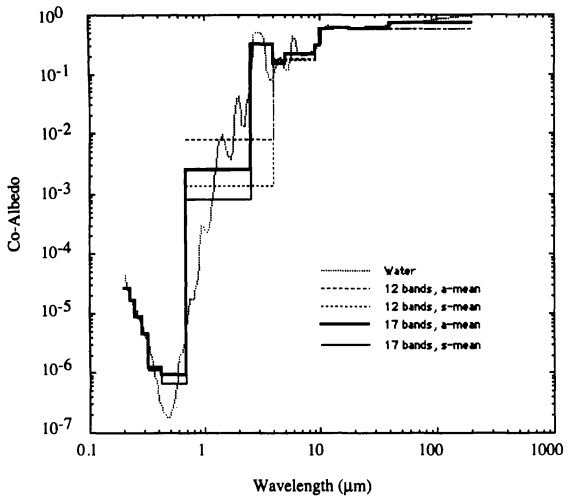

Fig. 11. Spectra of the co-albedo for several band allocations and a and s averages.

examples of a randomly overlapping cloud system. In this case, we put 1-km-thick clouds into all the sublayers with 1-km from 1 to 9 km, with $n = 0.5$ for all these sublayers. It is shown that the semirandom method slightly overestimates, by 0.03–0.05 K/day, the short-wave heating rate calculated by the random method. This error is smaller than the difference in heating-rate profiles for $n = 0.2$ and $n = 0$ shown in Fig. 9. This observation suggests that the proposed semirandom method is accurate enough to simulate random overlapping for our purpose, because there is more uncertainty in the validity of random overlapping in real atmospheres. Although this is not shown in a figure, the long-wave heating rate of randomly overlapping systems can be estimated quite accurately by the semirandom method. That this is so is understandable, as the formula is close to that of the random method when there is no scattering.

In our model, surface reflection and emission are introduced by a Lambert surface characterized by a flux albedo, A_g. For the ocean surface we fitted the empirical data of Payne[18] by the following formula to obtain the flux albedo:

$$A_g = \exp\left[\sum_{i=1}^{3}\sum_{j=1}^{5} C_{ij} t^i \mu_0{}^j\right], \tag{45}$$

where t is the flux transmissivity for short-wave radiation.

5. Discussion and Conclusion

It is not trivial to evaluate the band-averaged values of optical parameters in Eqs. (15) to attain the maximum efficiency for reducing the number of bands, because the absorption coefficient a_v of cloud particles is not so smooth a function in the NIR and IR spectral regions (Fig. 11). It is therefore worthwhile to consider the method of averaging to obtain band-

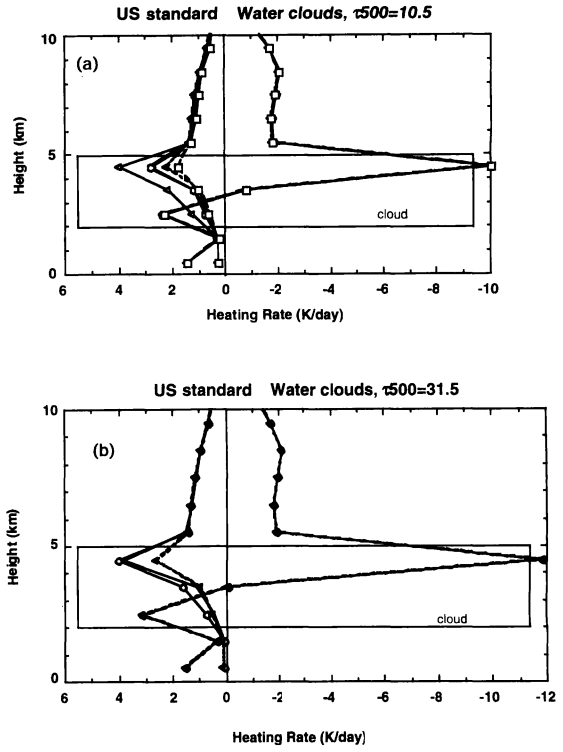

Fig. 12. (a) Comparison of heating-rate profiles calculated by several methods of averaging to obtain band-averaged parameters of particulate matter. The cloud optical thickness is 10.5. (b) Same as in (a) but with a cloud optical thickness of 31.5. ———, short-wave (sw) true (T); ——, long-wave (LW) T; true; —○—, SW 17-band a average; —○—, LW 17-band a average; —△—, SW 12-band a average; —△—, LW 12-band a average; —▲—, SW 17-band s average; —▲—, LW 17-band s average; —□—, SW 12-band s average; —□—, LW 12-band s average.

averaged parameters. For thin atmospheres the following average will be valid:

$$\langle e_v \rangle = \langle s_v \rangle + \langle a_v \rangle \approx s_v + \langle a_v \rangle, \tag{46}$$

where the angle brackets indicate wavelength integration over a band under consideration. For thick atmospheres, the similarity parameter $\xi = [(1 - \omega)/(1 - g\omega)]^{1/2}$ is an inherent parameter.[19,20] A highly variable factor for wavelength in the similarity parameter expression is $\sqrt{1 - \omega}$. We therefore can define an effective absorption coefficient $\langle a \rangle$ to conserve the wave-length average as follows:

$$\chi = \langle \sqrt{1 - \omega} \rangle \equiv [1 - \langle s \rangle / (\langle a \rangle + \langle s \rangle)]^{1/2}, \tag{47}$$

where $\langle s \rangle$ is the scattering coefficient averaged over a wavelength band. Then the expression for the effective absorption coefficient is

$$\langle a_v \rangle = \frac{\chi^2}{1 - \chi^2} \langle s_v \rangle. \tag{48}$$

We refer to those two averaging methods as a averaging and s averaging. As shown in Fig. 11, the co-albedo of clouds, $1 - \omega$, is smaller for s averaging than for a averaging. In Fig. 12, heating-

rate profiles with these averaging methods are compared for cloudy atmospheres. We put a cloud deck at 2–5 km into the U.S. Standard Atmosphere. For this case we used a four-stream approximation for a radiative transfer solution to identify the reason for the difference in these calculations. We tested 12-band (wave-number limits with 50, 550, 800, 980, 1100, 2500, 14 500, 24 000, 31 000, 35 000, 41 000, 45 000, and 50 000 cm^{-1}) models and 17-band 50, 250, 400, 550, 770, 990, 1100, 1400, 2000, 2500, 4000, 14 500, 24 000, 31 000, 35 000, 41 000, 45 000, and 50 000 cm^{-1}) models. The heating-rate profiles for long-wave radiation are well defined, without large deviations from the true value, even with the 12-band model. Band allocation is therefore not so critical for calculating the heating rate of cloudy atmospheres. However, Fig. 12 shows that short-wave heating rates depend on the number of bands used and on the method of averaging in a band. For the 12-band model there is only one NIR band, whereas the 17-band model has two NIR bands. It is shown, therefore, that one NIR band is not suitable for calculating short-wave fluxes. As for band averaging, *a* averaging is better than *s* averaging, except near the base of a thick cloud in the short-wave region. This is natural because *s* averaging is based on an asymptotic theory that is more suitable for thicker clouds.

As we have shown above, we are able to construct a fast yet comprehensive radiation code for use in climate modeling. We can treat scattering, absorption, and emission of particulate matter with the model as well as can gaseous absorption and emission without introducing an emissivity approximation and a band model. The amount of computation is proportional to the number of sublayers, owing to the discrete ordinate method/adding algorithm and a semirandom overlapping model. This advantage may compensate for the disadvantage that a large number of channels is needed for accurate calculation for a wide range of altitudes because recent GCM's tend to include more sublayers. Because our code, except for the transfer routine, does not depend on the number of quadrature streams, we easily can extend our code to a four-stream version by replacing the transfer routine. We also developed an objective method to determine parameters for the *k*-distribution method to maximize efficiency in reducing the number of channels. Although there are many problems to overcome to improve our method, we can conclude that our model is suitable and useful for climate modeling.

Appendix A

For a two-stream approximation, the formulas of Nakajima and Tanaka are reduced to scalar equations. The scaled reflection and transmission matrices are given as

$$R = \frac{1}{2}\left[\frac{X(1+E) - \lambda(1-E)}{X(1+E) + \lambda(1-E)} + \frac{X(1-E) - \lambda(1+E)}{X(1-E) + \lambda(1+E)}\right], \tag{A1a}$$

$$T = \frac{1}{2}\left[\frac{X(1+E) - \lambda(1-E)}{X(1+E) + \lambda(1-E)} - \frac{X(1-E)/\lambda - (1+E)}{X(1-E)/\lambda + (1+E)}\right], \tag{A1b}$$

where

$$X^{\pm} = \frac{1}{\mu}\{1 - [P^{(0)}(\mu, \mu) \pm P^{(0)}(-\mu, \mu)]w\},$$

$$X = X^{-}, \quad Y = X^{+}, \tag{A2}$$

$$G = XY, \quad \lambda = \sqrt{G}, \quad E = \exp(-\lambda\Delta\tau). \tag{A3}$$

where $\Delta\tau = \tau^{+} - \tau^{-}$ is the optical thickness of the layer.

Source vectors are

$$\varepsilon^{-} = V_0^{-} - RV_0^{+} - TV_1^{-}, \varepsilon^{+} = V_1^{+} - TV_0^{+} - RV_1^{-}, \tag{A4}$$

where vectors $V_0^{\pm}$ and $V_1^{\pm}$ are calculated as

$$\sigma_S^{\pm} = W^{-}\omega[P^{(0)}(\mu, \mu_0) \pm P^{(0)}(-\mu, \mu_0)], \tag{A5}$$

$$V_S^{\pm} = \frac{1}{2}\left[\left(1 \pm \frac{1}{X\mu_0}\right)\frac{\sigma_S^{+}X\mu_0 + \sigma_S^{-}}{G\mu_0 - 1/\mu_0} \pm \frac{\sigma_S^{-}}{X}\right], \tag{A6}$$

$$W^{-} = \sqrt{w/\mu}, \tag{A7}$$

$$c_n = 2\pi(1-\omega)W^{-}b_n, \tag{A8}$$

$$D_O^{\pm} = (2c_2/G + c_0)/Y \mp c_1/G,$$

$$D_1^{\pm} = c_1/Y \mp 2c_2/G, \quad D_2^{\pm} = c_2/Y. \tag{A9}$$

Then we have

$$V_0^{\pm} = V_S^{\pm}\exp(-\tau^{-}/\mu_0)F_0 + D_0^{\pm}, \tag{A10a}$$

$$V_1^{\pm} = V_S^{\pm}\exp(-\tau^{+}/\mu_0)F_0 + D_0^{\pm} + D_1^{\pm}\Delta\tau + D_2^{\pm}\Delta\tau^2. \tag{A10b}$$

From Eqs. (A5)–(A10), Eq. (A4) can be decomposed further into a term including the vector $V_S^{\pm}$ and a term including $D_i^{\pm}$:

$$\varepsilon^{\pm} = \varepsilon_S^{\pm}\exp(-\tau^{-}/\mu_0)F_0 + \varepsilon_B^{\pm}. \tag{A11}$$

The first term on the right-hand side of Eq. (A11) is a contribution of the solar radiation source, and the second term is that of the thermal radiation source. One can find ε_s and ε_B in Eq. (A4) by setting $\tau^{-} = 0$ and $F_0 = 0$ in Eqs. (A5)–(A10).

Appendix B

The scaled operators given in Appendix A for two sublayers can be combined to generate those for

added layers in a method that is similar to the ordinary matrix operator method:

$$R_{1,2}^{+} = R_1^{+} + T_1^{-}(I - R_2^{+}R_1^{-})^{-1}R_2^{+}T_1^{+},$$
$$T_{1,2}^{-} = T_1^{-}(I - R_2^{+}R_1^{-})^{-1}T_2^{-}, \tag{A12a}$$
$$\varepsilon_{1,2}^{-} = \varepsilon_1^{-} + T_1^{-}(I - R_2^{+}R_1^{-})^{-1}(R_2^{+}\varepsilon_1^{+} + \varepsilon_2^{-}). \tag{A12b}$$

We derive the operators $R_{1,2}^{-}$, $T_{1,2}^{+}$, and $\varepsilon_{1,2}^{+}$ in the same way by interchanging the roles of layers 1 and 2. The following expression for $\varepsilon_{1,2}^{-}$ is useful because we can utilize the expression of $\varepsilon_{1,2}^{+}$ for the calculation:

$$\varepsilon_{1,2}^{+} = \varepsilon_2^{+} + T_2^{+}[\varepsilon_1^{+} + R_1^{-}(I - R_2^{+}R_1^{-})^{-1} \times (R_2^{+}\varepsilon_1^{+} + \varepsilon_2^{-})]. \tag{A13}$$

Adding layers successively from bottom to top and then adding layers from top to bottom, we obtain the following internal intensities:

$$u^{+} = (I - R_1^{-}R_2^{+})^{-1}(R_1^{-}\varepsilon_2^{-} + \varepsilon_1^{+}),$$
$$u^{-} = R_2^{+}u^{+} + \varepsilon_2^{-}. \tag{A14}$$

We are grateful to Akihiro Uchiyama for providing us his line-by-line calculation code and for valuable discussions of calculating gas absorption spectra.

We dedicate this paper to the memory of our coauthor, Masahito Tsukamoto.

References

1. A. Lacis, W. C. Wang, and J. Hansen, "Correlated k-distribution method for radiative transfer in climate models: application to the effect of cirrus clouds on climate," NASA Conf. Publ. **2076,** 309–314 (1979).
2. M.-D. Chou, "A solar radiation model for use in climate studies," J. Atmos. Sci. **49,** 762–772 (1992).
3. Q. Fu and K. N. Liou, "On the correlated k-distribution method for radiative transfer in nonhomogeneous atmospheres," J. Atmos. Sci. **49,** 2139–2156 (1992).
4. K. Shibata and T. Aoki, "An infrared-radiative scheme for numerical models of weather and climate," J. Geophys. Res. **94,** 14,923–14,943 (1992).
5. T. Nakajima and M. Tanaka, "Matrix formulations for the transfer of solar radiation in a plane-parallel scattering atmosphere," J. Quant. Spectrosc. Radiat. Transfer **35,** 13–21 (1986).
6. J. H. Joseph, W. J. Wiscombe, and J. A. Weinman, "The delta-Eddington approximation for radiative flux transfer," J. Atmos. Sci. **33,** 2452–2459 (1976).
7. K. Stamnes, S.-C. Tsay, W. Wiscombe, and K. Jayaweera, "Numerically stable algorithm for discrete-ordinate-method radiative transfer in multiple scattering and emitting layered media," Appl. Opt. **27,** 2502–2509 (1988).
8. G. N. Plass, G. W. Kattawar, and F. E. Catchings, "Matrix operator theory of radiative transfer. 1. Rayleigh scattering," Appl. Opt. **12,** 314–329 (1973).
9. R. M. Goody and Y. L. Yung, *Atmospheric Radiation, Theoretical Basis*, 2nd ed. (Oxford U. Press, Oxford, 1989).
10. G.-Y. Shi, "An accurate calculation and representation of the infrared transmission function of atmospheric constituents," Ph.D. dissertation (Tohoku University, Sendai, Japan, 1981).
11. E. Raschke and U. Stucke, "Approximations of band transmission functions by finite sums of exponentials," Contrib. Atmos. Phys. **46,** 203–212 (1973).
12. A. Uchiyama, "Line-by-line computation of the atmospheric absorption spectrum using the decomposed Voigt line shape," J. Quant. Spectrosc. Radiat. Transfer **47,** 521–532 (1992).
13. F. X. Kneizys, E. P. Shettle, L. W. Abreu, J. H. Chetwynd, G. P. Anderson, W. O. Gallery, J. E. A. Selby, and S. A. Clough, "Users guide to LOWTRAN7, AFGL-TR-88-0177 (U. S. Air Force Geophysics Laboratory, Hanscom Air Force Base, Mass., 1988).
14. F. X. Kneizys, E. P. Shettle, W. O. Gallery, J. H. Chetwynd, Jr., L. W. Abreu, J. E. A. Selby, S. A. Clough, and R. W. Fenn, "Atmospheric transmittance/radiance: computer code LOWTRAN6, AFGL-TR-83-0187 (U. S. Air Force Geophysics Laboratory, Hanscom Air Force Base, Mass., 1983).
15. S. A. Clough, F. S. Kneizys, R. Davies, R. Gamache, and R. H. Tipping, "Theoretical line shape for H_2O vapor: application to the continuum," in *Atmospheric Water Vapor*, A. Deepak, T. D. Wilkerson, and L. H. Ruhnke, eds. (Academic, New York, 1980).
16. G.-Y. Shi, "Radiative forcing and greenhouse effect due to atmospheric trace gases," Sci. Sin. Ser. B **35,** 217–229 (1992).
17. J.-J. Morcrette and Y. Fouquart, "The overlapping of cloud layers in shortwave radiation parameterizations," J. Atmos. Sci. **43,** 321–328 (1986).
18. R. E. Payne, "Albedo of the sea surface," J. Atmos. Sci. **29,** 959–970 (1972).
19. T. Nakajima and M. D. King, "Asymptotic theory for optically thick layers: application to the discrete ordinates method," Appl. Opt. **31,** 7669–7683 (1992).
20. Harshvardhan and M. D. King, "Comparative accuracy of diffuse radiative properties computed using the selected multiple scattering approximation," J. Atmos. Sci. **50,** 247–259 (1993).